Geochronology of late Pleistocene to Holocene speleothems from central Texas: Implications for regional paleoclimate

MaryLynn Musgrove*
Jay L. Banner
Larry E. Mack
Deanna M. Combs
Eric W. James
Department of Geological Sciences, University of Texas, Austin, Texas 78712, USA

Hai Cheng
R. Lawrence Edwards
Department of Geology and Geophysics, University of Minnesota, Minneapolis, Minnesota 55455, USA

ABSTRACT

A detailed chronology for four stalagmites from three central Texas caves separated by as much as 130 km provides a 71 000-yr record of temporal changes in hydrology and climate. Mass spectrometric ^{238}U-^{230}Th and ^{235}U-^{231}Pa analyses have yielded 53 ages. The accuracy of the ages and the closed-system behavior of the speleothems are indicated by interlaboratory comparisons, concordance of ^{230}Th and ^{231}Pa ages, and the result that all ages are in correct stratigraphic order. Over the past 71 000 yr, the stalagmites have similar growth histories with alternating periods of relatively rapid and slow growth. The growth rates vary over more than two orders of magnitude, and there were three periods of rapid growth: 71–60 ka, 39–33 ka, and 24–12 ka. These growth-rate shifts correspond in part with global glacial-interglacial climatic shifts.

Paleontological evidence indicates that around the Last Glacial Maximum (20 ka), climate in central Texas was cooler and wetter than at present. This wetter interval corresponds with the most recent period of increased growth rates in the speleothems, which is consistent with conditions necessary for speleothem growth. The temporal shift in wetness has been proposed to result from a southward deflection of the jet steam due to the presence of a continental ice sheet in central North America. This mechanism also may have governed the two earlier intervals of fast growth in the speleothems (and inferred wetter climate). Ice volumes were lower and temperatures in central North America were higher during these two earlier glacial intervals than during the Last Glacial Maximum, however. The potential effects of temporal variations in precession of Earth's orbit on regional effective moisture may provide an additional mechanism for increased effective moisture coincident with the observed intervals of increased speleothem growth. The stalagmites all exhibit a large drop in growth rate between 15 and 12 ka, and they show very slow growth up to the present, consistent with drier climate during the Holocene. These results illustrate that speleothem growth rates can reflect the regional response of a hydrologic system to regional and global climate variability.

Keywords: caves, Edwards Plateau, geochronology, paleoclimate, speleothems, uranium-series method.

INTRODUCTION

The development of high-precision thermal-ionization mass-spectrometric techniques for uranium-series geochronologic measurements has resulted in significant advances in obtaining high-resolution records of sea-level change, terrestrial and marine climate, and the calibration of the ^{14}C time scale (e.g., Edwards et al., 1987, 1997; Chen et al., 1991; Gallup et al., 1994; Winograd et al., 1992; Dorale et al., 1998; Bard et al., 1990). Studies of calcite deposited from groundwater in caves (speleothems) and fracture fills have demonstrated the potential for speleothems to record high-resolution changes in groundwater chemistry, hydrology, and paleoclimatic variables (e.g., Li et al., 1989; Winograd et al., 1992; Gascoyne, 1992; Dorale et al., 1992, 1998; Bar-Matthews et al., 1997, 1999; Banner et al., 1996). Because Pleistocene through modern speleothems are precisely datable and can potentially yield continuous temporal and spatial sequences of growth, these speleothems may preserve continuous records of aquifer development and paleoclimatic parameters.

Constraints on growth rates and the timing of accelerated or slow growth in speleothems have provided insight into the timing of glacial and interglacial periods and related variables such as precipitation and effective moisture. Speleothem growth rates for multiple sites in Britain and northwestern Europe have been interpreted to document glacial-interglacial climate variability (e.g., Baker et al., 1993a, 1995a). In these temperate climates, speleothem growth can be limited during glacial periods by an ice-locked water supply and/or glacial cover that restricts recharge to the cave environment. In contrast, the present study documents speleothem growth in a region that was ice free during the glacial periods.

Speleothem growth is generally associated

*Present address: Department of Earth and Planetary Sciences, Harvard University, 20 Oxford Street, Cambridge, Massachusetts 01238, USA; e-mail: mlm@eps.harvard.edu.

GSA Bulletin; December 2001; v. 113; no. 12; p. 1532–1543; 6 figures; 1 table.

with an availability of moisture and recharge (e.g., Genty and Quinif, 1996; Railsback et al., 1994; Baker et al., 1995a; Brook et al., 1990). A review of published values indicates that speleothem growth rates may encompass several orders of magnitude of variability, from 0.0002 to 40 cm/yr (Hill and Forti, 1997). Given the dependence of geologic records of environmental change on an accurate and detailed chronology, we present rigorously assessed geochronologic data for late Pleistocene to Holocene speleothems from the Edwards aquifer region of central Texas. The results document the response of a regionally extensive hydrologic system to temporal shifts in climate. Variations in growth rates for central Texas speleothems provide a framework for evaluating the influence of climatic variations on aquifer development and long-term patterns of recharge.

HYDROLOGIC AND GEOLOGIC SETTING

The Edwards aquifer of central Texas is developed in Lower Cretaceous limestone and stretches in a narrow band along the Balcones fault zone (Fig. 1). Rainfall, which may vary significantly from year to year, is the primary source of aquifer recharge. Recharge is predominantly via losing streams as they cross the Balcones fault zone (Puente, 1975). Natural discharge occurs at springs within the fault zone. Tritium variations are consistent with groundwater residence times of 30 yr or less near the aquifer's recharge zone (Pearson et al., 1975). The Edwards Plateau has extensive karst development including many vadose caves and active calcite speleothem deposition (Elliott and Veni, 1994).

The climate of the Edwards Plateau becomes drier from east to west, with rainfall decreasing and evaporation rates increasing (Fig. 1). The variable climate and weather of the region is dominated by the balance of southerly to southeasterly air masses from the Gulf of Mexico and northerly continental polar air (Griffiths and Strauss, 1985). Dry and cool winters and hot summers characterize this drought-prone region. Approximately 85% of regional rainfall is lost to evapotranspiration (Burchett et al., 1986), which accounts for low effective moisture in the modern setting. Historical records of rainfall, recharge, and aquifer discharge indicate a clear link for the modern aquifer system between rainfall and effective moisture, which may be controlling the growth of speleothems.

Four stalagmite samples (DDS2, ISS2, CWN1, and CWN4) were collected from three caves that are up to 130 km apart on the eastern part of the Edwards Plateau (Fig. 1). These active caves are developed in the Lower Cretaceous Glen Rose Formation through the Lower Cretaceous Edwards Limestone. Owing to the similar physiographic location of the three caves with respect to the plateau, the area around the caves is characterized by similar variations in average annual temperature and rainfall (Fig. 1). The soils and vegetation of the region vary with effective moisture (Carter, 1931). Soils are predominantly developed from underlying limestones and are generally thin and stony, consisting of calcareous clay and clay loam (Kier et al., 1977). Although there are local variations, the soils and vegetation in the areas of the three caves are not significantly different (McMahan et al., 1984; Godfrey et al., 1973).

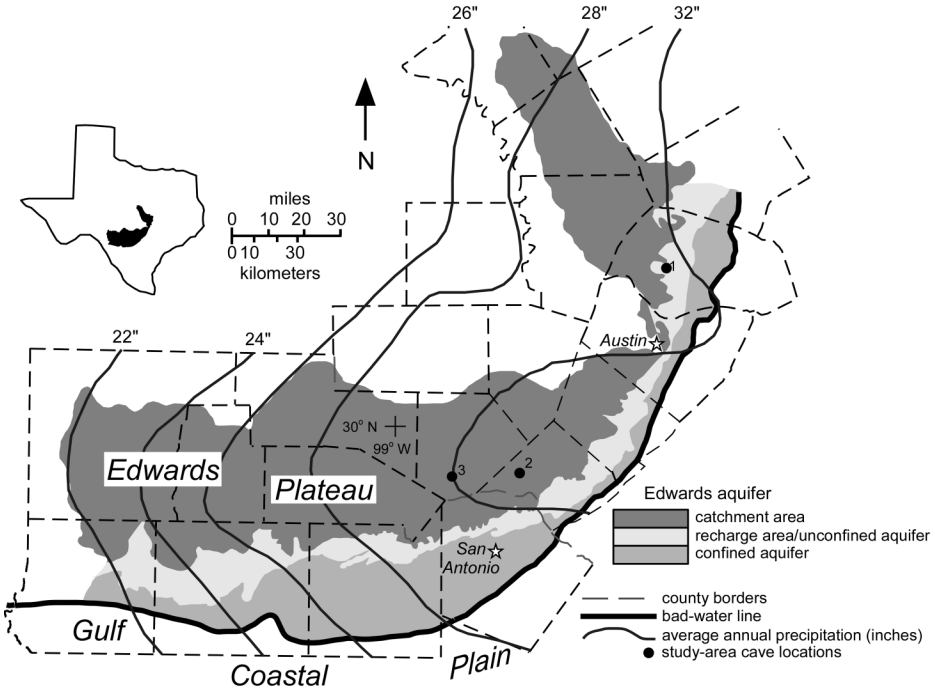

Figure 1. The hydrologic zones of the Edwards aquifer of central Texas; cave and sample locations are shown. Precipitation contours are from Larkin and Bomar (1983). The Balcones fault zone runs southwest to northeast and is approximated by the boundary between the catchment area and the recharge area/unconfined aquifer. The downdip limit of potable water in the aquifer is defined by the bad-water line (1000 mg/L). Caves in the study (filled circles): 1—Inner Space Cavern, 2—Double Decker Cave, and 3—Cave Without a Name. These caves are described in Elliott and Veni (1994).

METHODS

Age determinations were made by U-series isotope measurements on speleothem samples. Selected growth layers of calcite were drilled from the stalagmites, followed by chemical separation of U, Th, and Pa, and then by measurements of U-series isotopes by thermal-ionization mass spectrometry (TIMS) at the University of Texas at Austin (UT) and the University of Minnesota (UM). Because geochronology forms the basis of the present study and because these are the first U-series isotope results reported from UT, we present the details of our methodology (see the Appendix).

RESULTS

Reproducibility and Interlaboratory Comparisons

Uranium-thorium-protactinium (U-Th-Pa) isotope data, ^{230}Th ages, ^{231}Pa ages, and speleothem growth rates are given in Table 1. Replicate analyses (e.g., ISS2-I-d and ISS2-I-d-Rep.) were performed at UT on splits of powders from individual growth layers. Replicate/adjacent analyses were performed by collecting splits from directly adjacent growth layers (e.g., DDS2-K30-h and DDS2-K30-Adj.). Three of the four stalagmites (DDS2, ISS2, and CWN4) were dated with closely spaced age determinations (Fig. 2). Of 53 age

TABLE 1. URANIUM-SERIES DATA FOR CENTRAL TEXAS SPELEOTHEMS

Sample identification	Depth† (cm)	^{238}U (ppb)	±2σ	$\delta^{234}U$	±2σ	^{232}Th (ppt)	±2σ	$^{230}Th/^{238}U$ activity	±2σ	$^{230}Th/^{232}Th$ atomic (ppm)	±2σ	^{230}Th age (yr B.P.)	±2σ	Growth rate (mm/yr)	$^{231}Pa/^{235}U$ activity	±2σ	^{231}Pa age (yr B.P.)	±2σ
Double Decker Cave—Stalagmite 2																		
DDS2-Y-f	1.2	156	0.2	144.4	1.3	89.9	1.4	0.1504	0.0009	4320	70	15 290	110	0.0464				
DDS2-W	4.5	185	0.2	142.6	1.4	253	2	0.1572	0.0009	1900	20	15 990	160	0.0281				
DDS2-U*	7.9	135	0.2	171.6	3.6	48.4	6.8	0.1716	0.0027			17 200	300	0.0075	0.3166	0.0186	17 990	1290
DDS2-Q-f	11.4	125	0.2	179.8	1.5	107	2	0.2158	0.0017	4140	70	21 870	200	0.0251				
DDS2-M	16.4	89.40	1.37	239	29	812	3	0.2515	0.0049	460	4	23 860	1100	0.0009				
DDS2-L-35	17.3	59.90	0.06	215.3	1.9	740	2	0.3445	0.0025	460	4	35 030	1040	0.0007				
DDS2-L-30	18.2	71.81	0.08	230.2	1.4	235	2	0.4338	0.0026	2190	20	46 520	430	0.0016				
DDS2-L20-b	19.3	81.48	0.10	233.8	1.7	146	1	0.4877	0.0031	4510	50	53 810	470	0.0148				
DDS2-K30-h	26.4	93.84	0.17	242.0	1.7	96.2	1.3	0.5245	0.0037	8450	130	58 620	560	0.0038				
DDS2-K30 (Adj.)	26.7	90.82	0.15	236.9	1.7	169	1	0.5280	0.0035	4690	1	59 420	550	0.0370				
DDS2-K10-f*	31.7	92.70	0.20	234.2	4.5	67.7	7.5	0.5346	0.0029			60 640	550	0.0370	0.7311	0.0191	62 070	3360
DDS2-K10-c (Adj.)	32.1	89.58	0.32	245.7	2.4	35.8	1.5	0.5413	0.0037	22 350	930	60 880	570	0.1167				
DDS2-J	37.7	78.76	0.19	242.6	3.2	222	2	0.5443	0.0055	3190	40	61 360	880	0.0329				
DDS2-F-30	44.0	77.28	0.55	220.6	3.8	112	1	0.5458	0.0053	6250	90	63 260	880	0.0303				
DDS2-D	50.9	70.89	0.08	230.9	1.2	322	2	0.5671	0.0026	2060	20	65 550	540	0.0106				
DDS2-A-d	55.1	49.39	0.05	214.3	1.4	146	2	0.5823	0.0029	3260	40	69 460	540	0.0106				
Inner Space Cavern—Stalagmite 2																		
ISS2-Y	0.3	524	0.7	51.7	1.0	68.5	1.7	0.1260	0.0007	15 920	410	13 910	80	0.0038				
ISS2-V40	4.5	284	0.3	67.1	0.9	850	2	0.2209	0.0009	1220	6	24 990	300	0.0027				
ISS2-T60	6.7	362	0.7	62.8	1.7	15.6	1.5	0.2809	0.0016	107 650	10370	33 400	240	0.0909				
ISS2-T	8.7	509	1.3	64.8	2.3	247	2	0.2833	0.0012	9630	80	33 620	190	0.0234				
ISS2-S-f	10.9	560	0.8	64.4	1.0	26.5	1.8	0.2896	0.0011	101 040	6680	34 560	160	0.0289				
ISS2-R-i	12.6	583	0.7	61.9	0.9	64.8	2.2	0.2930	0.0014	43 540	1500	35 130	200	0.0005				
ISS2-Qq-R*	13.7	556	0.6	64.3	2.1	516	8	0.4334	0.0022			56 640	420	0.0030	0.7005	0.0137	56 990	2170
ISS2-Q	15.5	583	0.9	63.4	1.2	54.6	1.4	0.4666	0.0019	82 260	2070	62 640	370	0.0460				
ISS2-O	21.8	464	0.7	62.6	1.1	2720	10.0	0.4767	0.0016	1350	5	64 010	620	0.0782				
ISS2-I-d	30.4	452	0.9	63.3	1.5	8520	30	0.4943	0.0020	430	2	66 020	1800	0.0644				
ISS2-I-d (Rep.)	30.4	451	0.6	64.5	1.4	8720	30	0.4929	0.0025	420	2	65 590	1860	0.0644				
ISS2-H-n*	31.1	504	0.4	64.1	1.4	13 300	120	0.4987	0.0022			65 200	3350	0.0644	0.7302	0.0091	61 910	1600
ISS2-E	40.3	501	0.8	55.8	1.3	141	2	0.4895	0.0022	28 650	390	67 550	430	0.0278				
ISS2-A20-d	50.0	362	0.6	54.5	1.6	5530	20	0.5141	0.0018	560	3	71 060	1480	0.0278				
Cave Without a Name—Stalagmite 4																		
CWN4–11	0.4	273	0.4	356.3	1.3	9710	30	0.1221	0.0008	60	1	7650	2620	0.0031				
CWN4–10	2.0	254	0.3	353.4	1.3	2060	10	0.1565	0.0011	320	10	12 760	600	0.0198				
CWN4–9	4.2	459	0.6	350.6	1.3	255	2	0.1626	0.0008	4830	50	13 870	80	0.0417				
CWN4–8.05–1	7.2	324	0.3	344.8	1.1	1350	10	0.1724	0.0007	680	10	14 590	310	0.0296				
CWN4–8.05–1 (Rep.)	7.2	322	0.6	345.6	1.5	1180	10	0.1727	0.0007	780	10	14 630	280	0.0296				
CWN4–8	9.6	413	0.7	344.0	1.4	255	2	0.1783	0.0008	4780	40	15 400	90	0.0063				
CWN4–7	13.3	264	0.4	356.6	1.6	483	3	0.2434	0.0015	2200	20	21 280	190	0.0037				
CWN4–6	16.0	347	1.3	327.2	1.9	177	2	0.3084	0.0015	10 020	110	28 500	170	0.0211				
CWN4–5	20.7	426	0.6	339.2	1.2	137	2	0.3322	0.0013	17 100	250	30 730	140	0.0151				
CWN4–4	25.2	244	0.3	274.4	1.3	303	2	0.3428	0.0012	4570	40	33 720	140	0.0431				
CWN4–3.9*(Adj.)	25.6	246	0.3	237.1	3.1	121	11	0.3348	0.0017			34 060	230	0.0475	0.5256	0.0146	35 240	1460
CWN4–3	33.9	460	0.6	253.2	1.2	24.7	1.8	0.3534	0.0016	108 570	7810	35 740	150	0.0475				
CWN4–2	43.3	408	0.5	248.9	1.0	23.9	1.5	0.3686	0.0011	103 610	6320	37 720	140	0.0563				
CWN4–1.1*(Adj.)	47.6	480	0.5	248.2	1.7	203	7	0.3712	0.0016			38 030	230	0.0563	0.5522	0.0068	37 970	720
CWN4–1	47.8	476	0.6	249.6	1.3	316	2	0.3758	0.0013	9350	70	38 520	170	0.0563				
Cave Without a Name—Stalagmite 1																		
CWN-1–1B	1.5	391	0.4	344.2	1.3	2430	10.0	0.1684	0.0009	450	10	14 070	460	0.0444				
CWN-1–1A	17.5	364	0.4	291.0	1.2	564	3	0.1951	0.0008	2080	10	17 670	150	0.0444				

Notes: Growth rates were calculated by interpolating between dated growth layers. For example, the growth rate between DDS2-Y-F and DDS2-W is 0.0464 mm/yr. The growth rate between the uppermost sample and the stalagmite tip (not listed here, but shown in Fig. 4) was calculated by using an age and depth of zero. ^{230}Th ages corrected for initial $^{230}Th/^{232}Th$ as discussed in Appendix. All errors are 2σ of the mean. $\delta^{234}U$ is present-day value, as defined in Appendix.

*The six $^{231}Pa/^{235}U$ analyses were performed at the University of Minnesota.

†Refers to the distance of the sampled growth layer from the top of the sample.

determinations, all are in correct stratigraphic order with no age reversals. Age reversals in speleothems or any stratigraphically ordered sequence of samples are indicative of inaccuracies in either the analytical measurements or the corrections applied that account for the initial state of the system. Age reversals may also indicate diagenetic alteration (i.e., open-system behavior) or detrital contamination of the sample.

Ages from replicate analyses and analyses of directly adjacent growth layers agree within errors for intralaboratory analyses run at either UT (^{230}Th-^{230}Th age comparisons) or UM (^{230}Th-^{231}Pa age comparisons), as well as for comparisons between the two laboratories (^{230}Th-^{230}Th age comparisons). Replicate- and adjacent-sample results show that reproducibility for ^{232}Th concentration is lower than that of ^{230}Th ages, $[^{230}Th/^{238}U]_{Act}$ (the activity ratio of the given isotopes), $\delta^{234}U$, and ^{238}U concentrations (Table 1). This lower reproducibility likely reflects a heterogeneous distribution of ^{232}Th in the speleothems. The uncertainties in the ^{232}Th measurements have a negligible effect on the corrected ages reported in Table 1.

Pa and Th ages are concordant (Fig. 3). These are among the first reported mass-spectrometric ^{230}Th-^{231}Pa age comparisons for speleothems. Limited measurements of ^{231}Pa ages for speleothem materials have been previously performed by alpha spectrometry (Whitehead et al., 1999). Concordant TIMS analyses of the Devils Hole calcite (Edwards et al., 1997) and the results presented herein indicate that

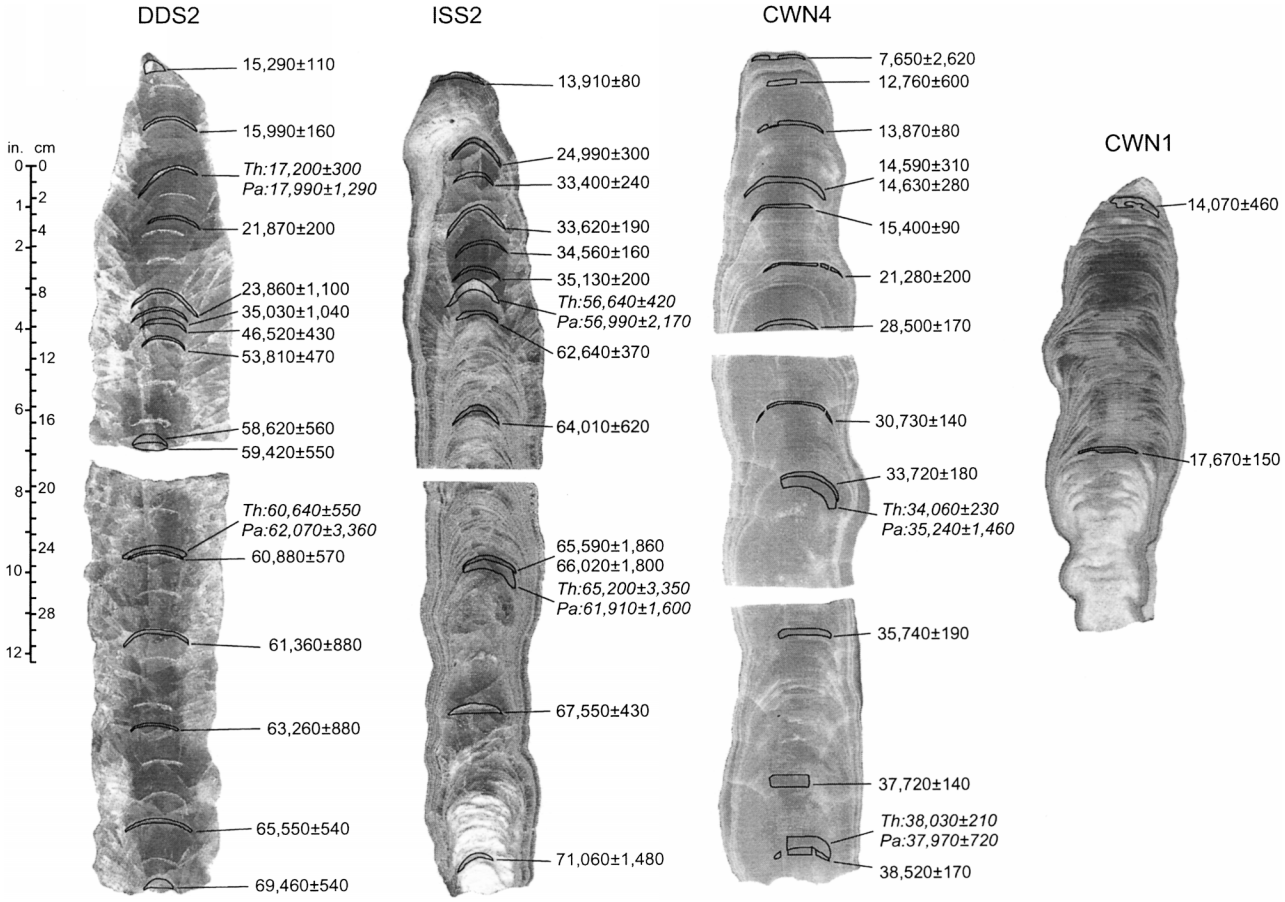

Figure 2. Stalagmite samples and geochronology. Stalagmites are composed predominantly of columnar calcite crystals. ISS2 contains areas of visible detrital material and columnar-fibrous fabric (based on the classification of Frisia et al., 2000). These areas were avoided when selecting growth layers for geochronology. Samples analyzed at the University of Minnesota are in italics. All ages are ^{230}Th ages unless otherwise noted.

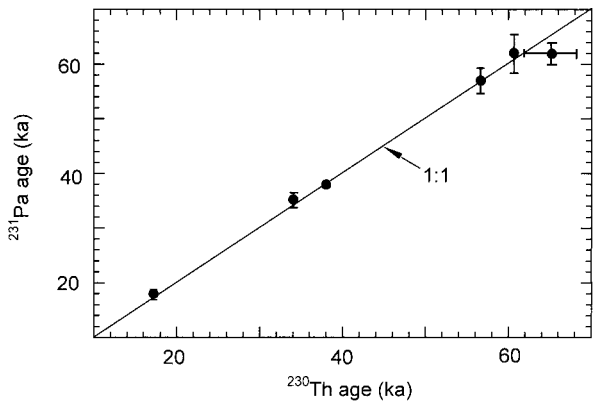

Figure 3. ^{230}Th age vs. ^{231}Pa age for six stalagmite growth layers. Comparisons to the 1:1 line illustrate the consistency of the two independent dating methods. All samples plot within error of the 1:1 line, which suggests that diagenesis has not shifted the pertinent parent:daughter isotope ratios and that corrections for initial ^{230}Th/^{232}Th are accurate within the given errors.

combined ^{230}Th-^{231}Pa dating is valid for cave-deposit and fracture-fill calcites and that the systems studied behave in a closed manner. The consistency of the sample and standard data between the two laboratories, concordant ^{230}Th-^{231}Pa ages, and lack of age reversals in this large data set all suggest that the ages and corresponding growth rates are accurate.

All pairs of ^{230}Th-^{231}Pa ages are concordant despite the fact that we have corrected for initial ^{230}Th, but not for initial ^{231}Pa. This fact suggests that corrections for initial ^{231}Pa are not significant compared to analytical error. This conclusion is not surprising given that ^{232}Th contents are low and therefore corrections for initial ^{230}Th are well below 1% for most samples. However, sample ISS2-H-n has a very high ^{232}Th content (Table 1) and a correspondingly large initial ^{230}Th correction (and hence a large age uncertainty), yet is concordant without a correction for initial ^{231}Pa. This relationship indicates that the high-^{232}Th component in the speleothem is low in ^{231}Pa. A

likely candidate for this component would be detrital clay from which Pa has been leached more strongly than has Th. This inference is reasonable given that Pa is less efficiently scavenged from seawater and therefore is generally more soluble than Th under surface conditions (Broecker and Peng, 1983).

Growth-Rate Variations

Growth rates are averaged between dated intervals by interpolation and are considered to be constant between dated points for the purpose of discussion. The four stalagmite samples exhibit growth rates that span more than two orders of magnitude (Table 1). In spite of this large range in absolute values, the stalagmite samples follow similar variations in temporal shifts and magnitudes of growth rates (Fig. 4). Two of the stalagmites are ca. 71 ka at their bases (DDS2 and ISS2), whereas records for CWN4 and CWN1 begin at 39 ka and 17 ka, respectively. Over the past 71 000 yr, the stalagmites preserved similar growth histories involving alternating periods of relatively rapid and slow rates of growth. Three periods of rapid growth occurred in the intervals 71–60 ka, 39–33 ka, and 24–12 ka. For the 39–33 ka period, sample DDS2 does not exhibit rapid growth. All four of the stalagmites had very slow apparent growth rates during the Holocene.

Some error in the calculated growth rates is introduced by averaging between dated intervals. This procedure may, in part, account for apparent differences in the timing of shifts in growth rates between samples. The large number of closely spaced age determinations, however, provides a rigorous analysis of growth-rate variations. The large range and frequent changes in growth rates determined for the central Texas stalagmite samples demonstrate that speleothem studies may require detailed geochronology. In addition to growth-rate variations, variations in trace-element abundances, stable isotopes of C and O, and radiogenic Sr isotopes may provide constraints on regional climatic and hydrologic processes (Musgrove, 2000). Oxygen isotopes in central Texas speleothems, however, likely do not provide a distinct record of relative paleotemperature or paleoprecipitation owing to the complexity of multiple factors that may affect the $\delta^{18}O$ of local rainfall in this subtropical region (Musgrove, 2000).

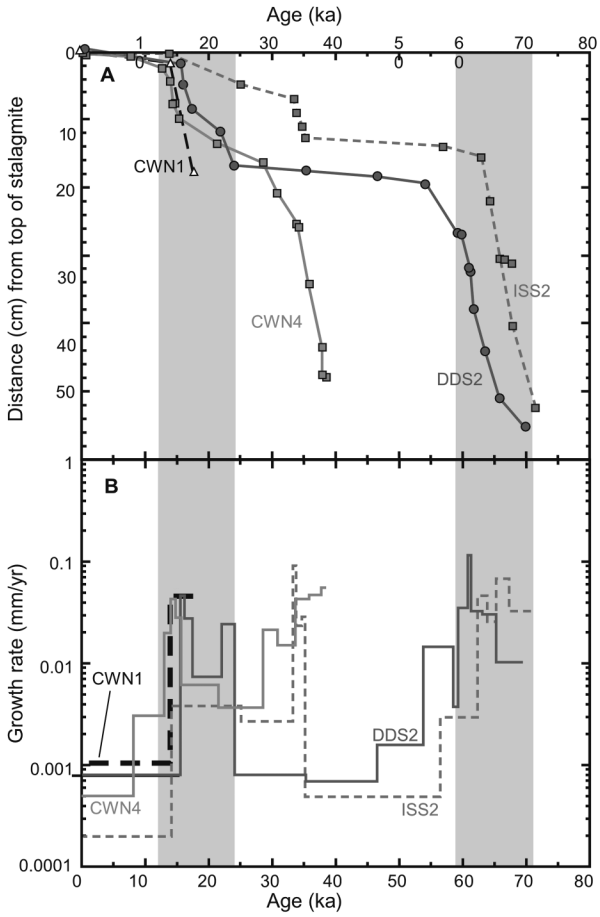

Figure 4. Growth rate histories for four central Texas stalagmites: (A) Growth-layer ^{230}Th age vs. depth of the growth layer from the stalagmite tip. The slope of the line for each sample represents the growth rate. Uncertainties on ages are given in Figure 3 and Table 1. (B) Calculated growth rate vs. time for the past 71 ka. Stepped curves are a result of interpolating constant growth rate between dated intervals. Shaded bands represent glacial intervals (marine oxygen isotope stages 2 [including the LGM between 20 and 14 ka] and 4 [left and right, respectively]) based on the time divisions of Imbrie et al. (1984).

FACTORS AFFECTING SPELEOTHEM CALCITE GROWTH

Speleothem growth is commonly driven by the degassing of calcite-saturated groundwater entering a cave (Holland et al., 1964). Although many factors may contribute to speleothem deposition, there are two overriding conditions that must be met: (1) CO_2 levels elevated above atmospheric values must be generated in the soil zone, and (2) water must be available for recharge (Baker et al., 1993a, 1995a). Carbon dioxide production in the soil zone generally decreases with cooler temperatures (Raich and Schlesinger, 1992; Raich and Potter, 1995). Thus, we infer that the primary condition promoting increased speleothem growth in the central Texas record during the last glacial period is increased moisture. It is also possible that in spite of cooler temperatures, the increased moisture during glacial intervals may have resulted in a positive feedback effect, resulting in greater soil productivity. Independent records for central Texas indicate that soils were thicker during the last glacial period (Toomey et al., 1993), which would be consistent with this possibility. In temperate regions, recharge will cease or slow if the ground is frozen, whereas in arid settings, recharge may only occur during wet periods. Regardless of the geographic setting, if little surplus water is available for recharge, speleothem growth will slow or stop.

Previous studies of young cave deposits in modern hydrologic systems, where climate records are available for comparison, provide evidence for a strong link between (1) the amount of rainfall and, correspondingly, the supply of infiltrating water feeding a speleothem and (2) speleothem growth (Railsback et al., 1994; Genty and Quinif, 1996). Although parameters such as evapotranspiration may

complicate this causal relationship, a link between the amount of rainfall and corresponding recharge is commonly observed in karst systems, including the Edwards aquifer of central Texas (Smart and Friederich, 1986; Musgrove, 2000). An understanding of these processes in modern systems provides a framework within which to interpret older speleothem growth records.

Studies of speleothem growth rates and climate have generally been applied to samples from high-latitude temperate regions, where glacial intervals are characterized by cool and dry conditions, in order to determine glacial versus interglacial conditions (e.g., Atkinson et al., 1978; Baker et al., 1993a, 1995a; Gordon et al., 1989; Gascoyne et al., 1983). A compilation of speleothem growth variations for multiple sites in Britain and northwestern Europe demonstrates a regionally consistent decrease in speleothem deposition during glacial intervals (Baker et al., 1993a). Thus, the presence or absence of speleothem growth during intervals of time may be used as a regional indicator of climatic conditions. In arid environments where little or no recharge occurs, speleothem growth may be limited to wetter and/or cooler intervals. The presence of speleothems in caves of modern-day deserts is indicative of speleothem deposition during wetter periods (Brook et al., 1990; Hennig et al., 1983).

The timing of growth phases in a flowstone from a cave in Britain demonstrates a close correlation between episodes of flowstone growth and solar insolation maxima (Baker et al., 1995a). Based on the effects of insolation on global circulation patterns, Baker et al. (1995a) inferred that insolation highs correspond to an increase in the intensity or amount of rainfall for the region, which in turn increases recharge to the speleothem. Thus, speleothem growth is sensitive to variations in rainfall and the nature of rainfall. However, a later comparison of these data with a coeval flowstone from a second cave less than 50 km away demonstrated only limited agreement (Baker et al., 1996). The differences between the two records were attributed to variations in local conditions between the two caves (Baker et al., 1996). The comparison of these samples suggests that it is prudent to integrate records from multiple sites to distinguish regional climatic signatures from local variations.

Consideration of the physical and chemical conditions of calcite precipitation has resulted in the development of a theoretical model for calcite deposition and speleothem growth (Dreybrodt, 1980; Buhmann and Dreybrodt, 1985a, 1985b). In this model, calcite precipitation is sensitive to calcium concentration, temperature, and drip rate; increases in these variables predict increased growth rate. Although it is difficult to determine these variables for any speleothem record, several points are noteworthy for the central Texas speleothem record.

Temperatures were likely several degrees lower in the region around the last glacial maximum (Toomey et al., 1993; Stute et al., 1992). The speleothem growth-rate model would predict decreased calcite precipitation rates as a result, owing to the temperature dependence of the rate constants for the conversion of CO_2 to HCO_3^- (Buhmann and Dreybrodt, 1985a, 1985b; Baker et al., 1998). The higher growth rates exhibited by the central Texas speleothem record during the last glacial maximum suggest that temperature does not appear to be a controlling factor for speleothem growth in the region over past 70 ka.

Calcite supersaturation must exist for speleothem deposition to occur. The interplay between calcium concentration and water supply may be complex (Baker and Smart, 1995; Baker et al., 1998). Modern drip waters in central Texas caves show no consistent correlation between drip rate and calcium concentration (Musgrove, 2000). The importance of calcium concentration may be a threshold-dependent parameter because calcite supersaturation may be maintained over a range of calcium concentrations and drip rates. Calcium concentration may become a controlling variable only when drip rates become so high that calcite supersaturation is no longer maintained; the system would then become calcium limited.

The link between increased water supply and speleothem growth rate is difficult to quantify, and the effects of changes in drip rate are modulated by site-specific variables. Application of the aforementioned theoretical growth-rate model to a Scottish speleothem growing over the past 7 ka estimated a 15% increase in growth rate with a doubling of the drip rate (Baker et al., 1995b). A study of modern speleothem growth in a Belgian sample over a 20-year period yields a more direct relationship, where a doubling of water supply results in an approximate doubling of growth (Genty and Quinif, 1996).

DISCUSSION

The correspondence of growth-rate trends for the four central Texas stalagmites indicates that growth-rate variations reflect a controlling mechanism on the spatial scale of the regional study area or even larger (Fig. 4). The main features of the growth histories are rapid growth during the periods 71–60 ka and 24–12 ka in all of the available speleothem records and during the period 39–33 ka for two of the three records. These rapid growth intervals are followed by periods of speleothem growth more than two orders of magnitude slower. The growth-rate record for the stalagmites correlates with a number of the global climatic shifts preserved in the marine oxygen isotope SPECMAP record (Fig. 5; Imbrie et al., 1984). Two distinct periods of increased growth rates are coincident with the timing of the last glacial period, marine oxygen isotope stage 2, and the preceding glacial interval, marine oxygen isotope stage 4 (Figs. 4 and 5). Very slow growth rates in the speleothems correspond to interglacial periods of the early part of marine oxygen isotope stage 3 and the current interglacial period of the past 12 000 yr. On the basis of the correspondence between speleothem growth and water supply already discussed, we propose that the consistent periods of increased stalagmite growth in central Texas are a result of a regionally wetter climate with higher effective moisture and a correspondingly increased water supply for stalagmite growth. The implications of this inference are discussed subsequently.

Regional Climate During the Last Glacial Period

Independent evidence indicates that during the Last Glacial Maximum (LGM), between 20 ka and 14 ka, climate in the central Texas region was both cooler and wetter than current conditions. This timing correlates with one of the periods of increased growth rates in the speleothems and is consistent with an increased water supply feeding stalagmite growth. Changes in both faunal remains and pollen and plant microfossil records in central Texas provide a continuous record of regional changes in climate, including effective moisture, over the past 20 000 yr (Fig. 6; Toomey et al., 1993; Bryant and Holloway, 1985). These data indicate that the region was cooler, with more effective moisture, during the last glacial period (20 ka to 14 ka) and underwent a subsequent warming and drying trend (13 ka to 10.5 ka), which continued through the Holocene and the modern semiarid and drought-prone climate (Toomey et al., 1993). A Pleistocene–Holocene transition to a drier climate, with less effective water for speleothem growth, is evident in the speleothem growth rates, which decreased markedly between 15 ka and 10 ka and remained low

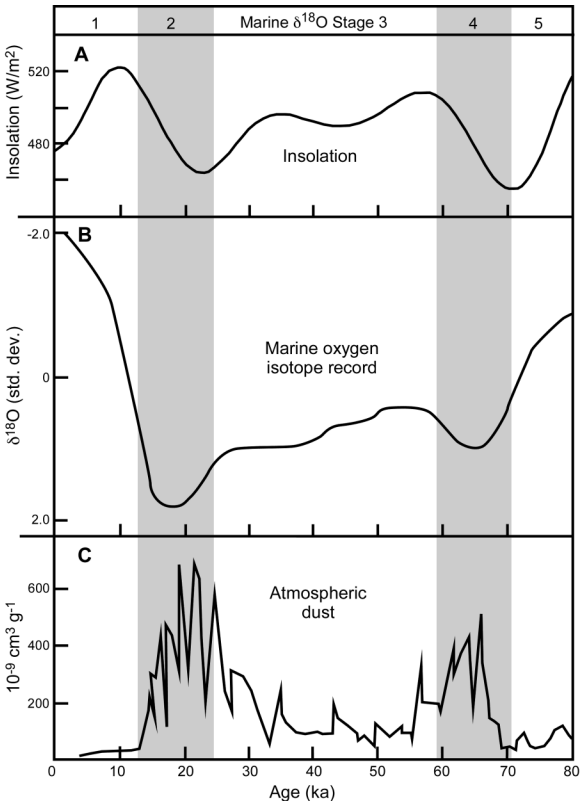

Figure 5. Compilation of select global climate records for 0 to 80 ka. Shaded bands represent glacial intervals (marine oxygen isotope stage 2 and 4) based on the time divisions of Imbrie et al. (1984). (A) Solar insolation record for 60° N from Berger and Loutre (1991). (B) Marine oxygen isotope SPECMAP record from Imbrie et al. (1984). Troughs (i.e., positive $\delta^{18}O$ standard deviations) in the SPECMAP record correspond with glacial intervals. (C) Record of atmospheric dust from the Vostok ice core (Jouzel et al., 1993).

throughout the Holocene (Fig. 4). A Pleistocene–Holocene transition to a drier climate is also supported by several other regional records. These include carbon isotope variations in pedogenic carbonates and humus and alluvial deposits from north-central and central Texas (Humphrey and Ferring, 1994; Nordt et al., 1994) and the fluvial landscape history of central Texas rivers (Waters and Nordt, 1995; Blum et al., 1994).

The integration of global climate records from marine sediments, ice cores, and loess indicates that, throughout the Quaternary, glacial periods have been characterized by drier and dustier Earth surface conditions (Petit et al., 1990; Jouzel et al., 1993). These effects are consistent with studies of speleothem growth rates already discussed for high-latitude climates that indicate less effective moisture and correspondingly decreased speleothem growth during glacial periods. Conversely, the speleothem growth-rate record for central Texas indicates that the region was wetter during the last glacial period and has become drier during the current interglacial. Toomey et al. (1993) proposed an explanation for this apparent contradiction based on atmospheric circulation patterns for the North American continent. Modern-day seasonal rainfall distribution across the western continental United States is strongly influenced by the position of the jet stream. A southward shift or splitting of the mean jet stream position results in dry conditions in the northwest and wet conditions in the southwest (Thompson et al., 1993). Early studies of the Great Basin suggested that a large continental ice sheet over North America may affect the mean position of the jet stream, resulting in its deflection to the south, which would bring increased year-round moisture to the southwest (Antevs, 1952). The presence of extensive pluvial lakes in basins of the western United States during the last glacial period is well-documented (Smith and Street-Perrott, 1983; Benson and Thompson, 1987; Benson et al., 1990). An increase in moisture supplied to the southwestern United States during the last glacial period is consistent with a southward deflection of the jet stream and extensive pluvial lakes. The presence of permanent lakes in New Mexico and west Texas during the last glacial period provides additional evidence of a regionally cooler and moister (i.e., pluvial) climate (Allen and Anderson, 1993; Wilkens and Currey, 1997; Reeves, 1973). Furthermore, major highstands for lakes in the Trans-Pecos closed basin of west Texas and south-central New Mexico during the last glacial maximum are synchronous with highstands of lakes in central New Mexico (Wilkens and Currey, 1997).

Studies of pluvial lakes in the southwestern United States have investigated whether the increase in moisture is a result of (1) lower temperatures, (2) increased rainfall, or (3) a combination of the two. An analysis of the large southwestern pluvial lakes of the last glacial period concludes that during the pluvial maxima associated with the LGM, most streams in the western United States carried as much as an order of magnitude greater streamflow, groundwater tables were higher, and precipitation was markedly increased (Smith and Street-Perrott, 1983). Numerical modeling experiments addressing the water balance of western lake basins indicate that changes in the water balance are driven more by precipitation variations than temperature (Phillips et al., 1992). A southward deflection of the jet stream during the last glacial maximum would result in more frequent winter storms across the western and southwestern United States. This increased winter precipitation was likely the most effective means of maintaining high paleolake levels in the Great Basin and the southwestern United States (Benson and Thompson, 1987), as well as increased moisture in central Texas.

Regional and Global Glacial Climates

In addition to lake-level data, other studies support the presence of greater effective moisture and a wetter climate in the Great Basin and southwestern United States during the last glacial period (marine oxygen isotope stage 2). Although many of these records do not extend back to marine oxygen isotope stage 4, there are still a number of indicators that consistently point to a wetter climate during this period. U-series dating of travertine deposits in Grand Canyon National Park, Arizona, which are inferred to have formed during periods of greater effective moisture, indicate intervals of deposition centered at ca. 15 and 71 ka (Szabo, 1990). Water-table fluctuations in southern Nevada have been reconstructed

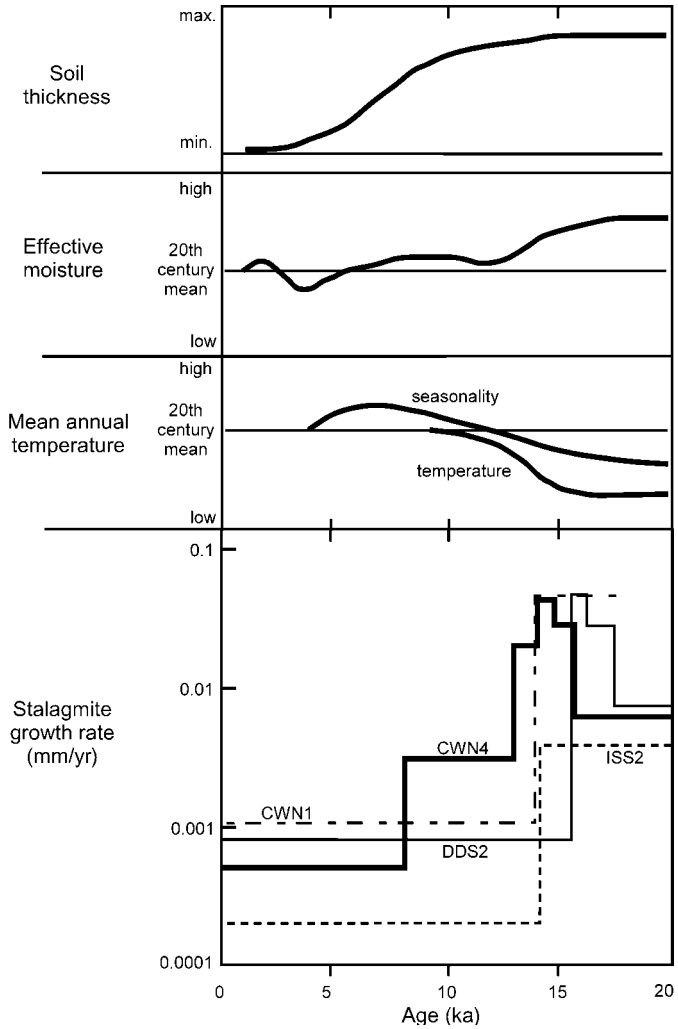

Figure 6. Compilation of independent regional climate records for central Texas compared with the speleothem record for 0 to 20 ka. Climate records indicate a transition to more arid conditions at the Pleistocene-Holocene boundary, which is consistent with the marked decrease in speleothem growth rates. Trends for soil thickness, effective moisture, temperature, and seasonality from Toomey et al. (1993).

from calcite deposits precipitated in a subterranean chamber connected to Devils Hole that indicate similar timing for higher water levels (i.e., stages 2 and 4) resulting from a wetter climate in this groundwater basin (Szabo et al., 1994). The Devils Hole vein calcite record shows relatively low $\delta^{18}O$ values at ca. 65 ka, correlative with marine oxygen isotope stage 4 (Winograd et al., 1992). Groundwater residence times in the regional aquifer supplying water to Devils Hole may have been significantly reduced during glacial climates as a result of increased aquifer recharge that flushed groundwater more quickly through the system (Winograd et al., 1988). U-series ages of speleothems from Carlsbad Caverns, New Mexico, indicate that speleothem growth was more rapid during glacial stages over the past 175 ka (Brook et al., 1990; Eubanks et al., 1985).

Results of general circulation model (GCM) simulations investigating the influence of continental ice sheets on atmospheric circulation and on climate-system boundary conditions support the concept of a southward deflection of the jet stream over North America during the last glacial period and a displacement of storm tracks far to the south (Manabe and Broccoli, 1985; Kutzbach and Guetter, 1986; Kutzbach and Wright, 1985; Rind, 1987; COHMAP Members, 1988). GCM studies also suggest that mean annual soil moisture was greater in the western United States and Mexico during the LGM (Broccoli, 2000).

Our data suggest that climate in central Texas was wet during marine oxygen isotope stages 4 and 2. Unfortunately, glaciations tend to obliterate evidence of their precursors. Thus, the record of the extent of the stage 4 glaciation of North America is not as clear as the record for the more recent stage 2. Although their geographic extent remains unclear, the presence of stage 4 (early Wisconsinan) ice sheets in North America is supported by independent data from glacial deposits in the Sierra Nevada and Quebec (Phillips et al., 1990; Lamothe et al., 1992). Additionally, there is evidence that lake levels in the Great Basin were high during stage 4 (Oviatt and McCoy, 1992). We therefore infer that the relationship documented for marine oxygen isotope stage 2 that links (1) a wetter climate in central Texas, (2) Great Basin pluvial lakes, (3) a continental North American ice sheet, and (4) the southward deflection of the jet stream also played at least a partial role during stage 4. On the basis of the marine oxygen isotope record, however, this interval was a period of lower continental ice volume than stage 2. This interval was also a period of changing ice volume from relatively high volume during marine oxygen isotope stage 4 to relatively low volume during the early part of stage 3 (Fig. 5). During this shift to low ice volume, central Texas speleothem growth rates slowed significantly. Global ice volume may have increased slightly during the middle of stage 3, which corresponds with an increase in speleothem growth rates (Figs. 4 and 5). Thus, the positive correlation between ice volume and speleothem growth rates, which we observe for marine oxygen isotope stage 2, also seems to hold for stages 3 and 4. Continental ice volume was lower for stages 3 and 4, however, relative to stage 2. For this reason, the southward deflection of the jet stream (associated with high ice volume) may not be the sole cause of high growth rates.

During the latter part of stage 3, an increase in growth rate is evident in two of the stalagmite samples, CWN4 and ISS2, between 39 and 33 ka (Fig. 4). Sample DDS2, however, does not exhibit this increase. The coincident increase in growth rates during this period (39 ka to 33 ka) recorded in two of the stalagmites may reflect regional and correspondingly global climatic parameters that are not recorded in DDS2 owing to some change in local hydrologic variables that are inconsistent between the caves. Several independent lines of evidence indicate that the growth-rate increase during this time may reflect climatic parameters of at least regional scale. The oxygen isotope record at Crevice Cave, Missouri (Dorale et al., 1998), is the closest climate record with

resolution, length, and age control similar to records analyzed in central Texas. The Crevice Cave record shows cool to warm climatic shifts centered at 64 and 37 ka, which correspond with the two earlier intervals of higher speleothem growth in central Texas. There is also evidence for high lake levels in the Great Basin for the 39 to 33 ka period, which, as already discussed, is consistent with a wetter climate in central Texas. Although some Great Basin lakes were at low levels around 35 ka, there is evidence that Lake Russell and Lake Searles were at moderate levels, and then dropped off by 33 ka (Benson et al., 1990). An expansion of Searles Lake in southeastern California at 34 ka has been correlated with a Greenland Summit ice-core interstadial and proposed to be linked by increased precipitation (Phillips et al., 1994).

Variations in solar insolation may also contribute to fluctuations in rainfall and effective moisture in the central Texas region. The three temporal intervals of faster central Texas stalagmite growth occurred during an orbital configuration when the longitude of the perihelion is in spring (March 17 at 65.5 ka, May 17 at 36 ka, and March 4 at 18 ka, respectively; C. Jackson, 2001, personal commun.). Examination of a low-resolution atmosphere-slab ocean climate system model's response to continuous changes in orbital forcing over the past 165 ka (C. Jackson and A.J. Broccoli, 2001, personal commun.) shows that precession (more so than obliquity) is an important orbital parameter influencing seasonal changes in Texas precipitation and soil moisture. The model shows that a spring perihelion in central Texas leads to (1) a seasonal late-fall and early-winter increase in rainfall and (2) a maximum in soil moisture during the same seasons. During these seasons, cooler temperatures would favor recharge because of decreased evaporation. In contrast, during the Holocene, when the stalagmites exhibited slow growth rates, the longitude of the perihelion has gradually migrated from summer to winter (July 13 at 10 ka to January 1 at present). The observed association of spring perihelion and speleothem growth indicates that the Holocene range of orbital configurations would favor relatively slow speleothem growth. In summary, the speleothem growth-rate record may reflect the climate system's response to precessional forcing. More work is needed to clarify the relevance of this model's results, especially given the large changes in ice-sheet extent over the past 71 ka, which are not incorporated into the model's design.

With respect to the individual central Texas stalagmite records, the following question remains: If the fast growth rates recorded in CWN4 and ISS2 between 39 and 33 ka are reflecting a regional or global event, why is the same event not recorded by increased growth rates in DDS2? The growth-rate record of the speleothems ultimately reflects a combination of climate and hydrology, both regional and local, that is specific to the flow-routing of each stalagmite and each cave. Temporal changes in soil thickness across the Edwards Plateau (Toomey et al., 1993) may also affect recharge processes. Given these complexities, the approach used herein of integrating multiple samples and/or multiple caves may best allow for delineating a regional picture of the hydrologic response to climate variability.

SUMMARY AND IMPLICATIONS

The central Texas speleothem growth record for the past 71 ka represents the first continuous regional climate record for central Texas extending beyond the Last Glacial Maximum. A greater than two-orders-of-magnitude range in stalagmite growth rates appears to reflect variations in effective moisture supplied to the stalagmites. Three intervals in the past 71 ka were characterized by a wetter climate, evidenced by increased speleothem growth rates in the region. Speleothem growth slowed markedly during the climate transition at the Pleistocene–Holocene transition and remained very low throughout the Holocene, indicative of a pronounced shift to a drier climate. These results are consistent with independent climate records.

The results of this study indicate that speleothem growth rates determined by high-resolution geochronology have application for reconstructing regional climatic conditions. Variability in individual stalagmite samples shows the necessity of an approach that integrates data from multiple samples and multiple sites in order to distinguish a response to regional variability versus local conditions. Large variations in speleothem growth rates indicate that detailed geochronology is necessary to accurately determine temporal constraints on climate records from speleothems. Concordant ^{230}Th-^{231}Pa age determinations suggest the potential for accurate age dating and the closed-system behavior of these types of geologic materials.

APPENDIX

ANALYTICAL METHODS

U and Th isotope analyses were conducted at the University of Texas at Austin (UT), and Pa and Th comparisons were conducted at the University of Minnesota (UM). The methods described here refer to those used at UT, except where indicated otherwise.

Sample Selection

All of the samples analyzed are stalagmites. Those selected for this study have a simple stratigraphy, low porosity, and relatively low common-Th (i.e., ^{232}Th) concentrations (Table 1). Prior to their collection, the stalagmites had been broken during cave development or by vandalism, likely within the past 50 years. Stalagmites were cut along their growth axes and polished by using a water saw and diamond lapidary wheels. Polished samples and thin sections were evaluated for porosity and detrital contamination and were inspected petrologically to screen for recrystallization textures and/or growth hiatuses marked by detritus and/or dissolution surfaces. Porous and permeable calcite may be susceptible to postdepositional alteration by leaching, cementation, or adsorption due to increased surface area, or may house detrital material (Ivanovich and Harmon, 1992). Detrital material within the calcite may contribute excess ^{230}Th to the sample and yield an apparent older age (Schwarcz and Latham, 1989). Growth layers with low porosity and low amounts of detrital material were preferentially selected for geochronology. From a selected growth layer, ~1 g was sampled by using a dental drill with carbide-tipped burrs and a binocular microscope, housed within a class-100 environment. These powdered samples were microscopically examined for foreign particles and detrital material, which were subsequently removed.

Chemical Separation

Chemical separation procedures followed those detailed in Edwards et al. (1987, 1993) and Cheng et al. (2000). Samples were dissolved in concentrated HNO_3, then spiked with ^{229}Th and mixed ^{233}U-^{236}U (^{233}U ≅ ^{236}U) tracers. U and Th tracer solutions were calibrated by using gravimetric solutions of New Brunswick Laboratories (NBL) Standard Reference Material 112-A (formerly NBS U960) and purified Th metal prepared by the Standard Materials Preparation Center at Ames Laboratory, Iowa, respectively. U and Th were coprecipitated from the mixed sample-tracer solutions with $Fe(OH)_3$ and purified by ion-exchange chemistry. A two-column separation (750 μL and 160 μL) was performed by using Bio-Rad anion exchange resin AG1 X8, 100–200 mesh. Yields are ~90% for both U and Th. Total procedural blanks (chemistry plus filament loading) are ≤4.0 pg for U and ≤2.0 pg for Th.

Mass Spectrometry

U and Th isotope analyses were conducted at UT on a Finnigan-MAT 261 thermal-ionization mass spectrometer (TIMS) upgraded with an ion-counting detection system using a MasCom secondary-electron multiplier (SEM). U and Th separates were loaded onto zone-refined Re filaments (prescreened for Th content) with colloidal graphite and run in single-filament configuration. All masses were measured by using the ion-counting system. Ionization efficiencies for Th average 0.4‰. Instrumental fractionation of U isotopes was corrected by using the ^{233}U/^{236}U ratio of the tracer. The range of fractionation values observed for U measurements is α

$= -3.2‰$ to $+1.5‰$ per AMU (atomic mass unit; mean $= -0.8‰$; $n = 73$). Applying this range of fractionation values to the Th isotope measurements has a negligible effect relative to the analytical uncertainty. In addition, the change in Th isotope ratios during the course of an analysis is less than the analytical uncertainty. Thus, Th isotope ratio measurements are not normalized for instrumental fractionation.

Abundance sensitivity (tail at mass 237/peak at mass 238) varied within the range 0.6 to 1.1 ppm during the course of this study. To determine the effects of tailing from the large ^{238}U and ^{232}Th peaks, baselines in the U and Th mass range were profiled in detail under varying run conditions. For the U mass spectrum from 232.5 to 237, the shape of the background between adjacent background positions follows a linear model and allows precise interpolation and extrapolation of backgrounds from measurements at 233.5, 234.4, and 235.5. Following the similar procedures for analysis of the Th mass spectrum, backgrounds are measured at 229.5.

Mass bias in the SEM was determined (following Cheng et al., 2000) to be $0.1 \pm 0.6‰$ and $0.1 \pm 0.2‰$ per AMU (lower mass is overcounted), respectively, for the two SEMs used during the course of this study. Normalization for U fractionation also accounts for mass bias, and consequently a mass bias correction is applied only to Th measurements. The effects of dead time and intensity bias were calibrated by measurements on isotope standards over a range of ion-beam intensities, and a correction for these effects was made to all measurements. The uncertainties associated with the corrections for instrumental fractionation, analytical blanks, backgrounds, mass bias, intensity bias, and dead time are small compared with the overall analytical uncertainty on the U and Th isotope ratio measurements.

Ages were calculated by using the $^{230}Th/^{238}U$ decay equation for closed U-Th systems (Broecker, 1963):

$$\left[\frac{^{230}\mathrm{Th}}{^{238}\mathrm{U}}\right]_{\mathrm{Act}} = 1 - e^{-\lambda_{230}\times T} + \left(\left[\frac{^{234}\mathrm{U}}{^{238}\mathrm{U}}\right]_{\mathrm{Act}} - 1\right) \times \left(\frac{\lambda_{230}}{\lambda_{230} - \lambda_{234}}\right) \times (1 - e^{-(\lambda_{230}-\lambda_{234})\times T}). \quad \text{(A1)}$$

$[^{230}Th/^{238}U]_{Act}$ and $[^{234}U/^{238}U]_{Act}$ indicate the activity ratios and T is the ^{230}Th age. Values for decay constants λ_{230}, λ_{234}, and λ_{238} used are 9.1577×10^{-6} y^{-1} (Cheng et al., 2000), 2.8263×10^{-6} y^{-1} (Cheng et al., 2000), and 1.55125×10^{-10} y^{-1} (Jaffey et al., 1971), respectively. The ^{230}Th ages and uncertainties reported in Table 1 include analytical errors (which are between $\pm 0.4\%$ and 1% for all except five samples), as already discussed, and corrections for initial ^{230}Th abundance at the time of calcite growth. Age corrections for initial ^{230}Th were calculated by using a sample's measured ^{232}Th concentration and an assumed initial $^{230}Th/^{232}Th$ ratio of $1.5 (\pm 1.5) \times 10^{-5}$. This ratio is a more conservative estimate of initial $^{230}Th/^{232}Th$ than the commonly used ratio of $4.4 (\pm 4.4) \times 10^{-6}$ (the value for a material at secular equilibrium with an average crustal $^{232}Th/^{238}U$ value of 3.8; e.g., Banner et al., 1991; Dorale et al., 1998). The $1.5 (\pm 1.5) \times 10^{-5}$ value is determined by the ages and stratigraphic order of neighboring samples. The corrections to a sample's ^{230}Th age and its associated uncertainty for initial $^{230}Th/^{232}Th$ are smaller than the analytical errors for most samples. Sample ISS2-H-n is the most notable exception, with an error of 5%, because of the high ^{232}Th content of this sample (Table 1). The uncertainty in ^{230}Th age that is introduced by the uncertainty in the initial $^{230}Th/^{232}Th$ value is greater for samples with high ^{232}Th contents and for younger samples (e.g., CWN 4–11), for which the fractional error in age introduced by the correction may be large compared to the amount of radiogenic ^{230}Th. Analysis of modern speleothem calcite, the insoluble residues of speleothem calcite, and modern cave drip waters will place more rigorous constraints on initial $^{230}Th/^{232}Th$ values.

NBL Standard Reference Material 112-A was used as a U standard. Uranium isotope compositions are reported as $\delta^{234}U$ in per mil notation:

$$\delta^{234}\mathrm{U} = \{[(^{234}\mathrm{U}/^{238}\mathrm{U})/(^{234}\mathrm{U}/^{238}\mathrm{U})_{\mathrm{eq}}] - 1\} \times 10^3. \quad \text{(A2)}$$

$(^{234}U/^{238}U)_{eq}$ is the atomic ratio at secular equilibrium and is equal to $\lambda_{238}/\lambda_{234}$. Note that our $\delta^{234}U$ values are calculated with a recently determined λ_{234} value (Cheng et al., 2000), which gives a $\delta^{234}U$ value about 3‰ lower (for materials close to secular equilibrium) than values calculated by using earlier decay constant values (e.g., those used in Edwards et al., 1987). Thirty-three measurements of NBL-112A over the three-year course of this study yield a mean $\delta^{234}U$ value of $-37.0‰ \pm 3.2‰$ (error = external 2σ). This compares with values reported from the University of Minnesota of -37.1 ± 1.2 ‰ ($n = 8$, error = external 2σ, Edwards et al., 1993, recalculated with the Cheng et al., 2000, λ_{234} value) and $-36.9‰ \pm 2.1‰$ ($n = 21$, error = external 2σ, Cheng et al., 2000). In terms of accuracy, the UT value is in agreement with the true isotope value of NBL-112A (-36.9 ± 1.7, $2\sigma_{mean}$ of 21 measurements plus systematic errors; Cheng et al., 2000) and is also in agreement within error with values reported by other laboratories (e.g., Chen et al., 1986; Goldstein et al., 1991; Stirling et al., 1995).

^{235}U-^{231}Pa Analysis

In order to test the accuracy of the ^{230}Th ages, six additional samples were analyzed for both ^{230}Th ages and ^{231}Pa ages at UM. The combined ^{231}Pa and ^{230}Th systems provide two independent chronometers, analogous to those of the U-Pb system, which can potentially be used to determine the extent of diagenetic alteration (Edwards et al., 1997; Cheng et al., 1998). ^{231}Pa ages are based on the radioactive decay of ^{235}U to ^{231}Pa (half-life = 32 760 yr; Robert et al., 1969). The ^{231}Pa age equation is (Ku, 1968)

$$\left[\frac{^{231}\mathrm{Pa}}{^{235}\mathrm{U}}\right]_{\mathrm{Act}} = 1 - e^{-\lambda_{231}\times T}. \quad \text{(A3)}$$

Samples analyzed for U-Pa were also analyzed for U-Th at UM so that comparisons between the dating systems could be made on the same solution. Pa procedures are those of Pickett et al. (1994), modified as described by Edwards et al. (1997). U-Th analyses are modifications of those of Edwards et al. (1987), as described in Edwards et al. (1993) and Cheng et al. (2000). Calcite samples of ~3 g were dissolved and divided into two aliquots, one for Pa analysis and one for U-Th analysis. The Pa aliquot was spiked with a ^{233}Pa tracer milked from a solution of ^{237}Np. The Pa, U, and Th fractions were isolated by $Fe(OH)_3$ coprecipitation and ion-exchange chemistry and run on a Finnigan MAT-262-RPQ TIMS. Both Pa and Th were run on single zone-refined rhenium filaments with colloidal graphite. Uranium was run by using double rhenium filaments without graphite.

ACKNOWLEDGMENTS

We thank the management and owners of Inner Space Cavern, Cave Without a Name, and Double Decker Cavern, and E. Lundelius for access to caves and logistical assistance with this project. Helpful reviews by C. Jackson, L. Stern, T. Ku, Associate Editor C. Johnson, and an anonymous reviewer improved the manuscript. We thank C. Jackson for climate model results and generous and insightful discussion. This research was supported by the Department of Energy (DE-FG03–97ER14812), the National Science Foundation (EAR-9526714), the Environmental Protection Agency (915135–01), the Cave Conservancy Foundation, and the Geology Foundation of the University of Texas at Austin.

REFERENCES CITED

Allen, B.D., and Anderson, R.Y., 1993, Evidence from western North America for rapid shifts in climate during the Last Glacial Maximum: Science, v. 260, p. 1920–1923.

Antevs, E., 1952, Cenozoic climates of the Great Basin: Geologische Rundschau, v. 40, p. 94–108.

Atkinson, T.C., Harmon, R.S., Smart, P.L., and Waltham, A.C., 1978, Palaeoclimate and geomorphic implications of $^{230}Th/^{234}U$ dates on speleothems from Britain: Nature, v. 272, p. 24–28.

Baker, A., and Smart, P.L., 1995, Recent flowstone growth rates: Field measurements in comparison to theoretical predictions: Chemical Geology, v. 122, p. 121–128.

Baker, A., Smart, P.L., and Ford, D.C., 1993a, Northwest European palaeoclimate as indicated by growth frequency variations of secondary calcite deposits: Palaeogeography, Palaeoclimatology, Palaeoecology, v. 100, p. 291–301.

Baker, A., Smart, P.L., Edwards, R.L., and Richards, D.A., 1993b, Annual growth banding in a cave stalagmite: Nature, v. 364, p. 518–520.

Baker, A., Smart, P.L., and Edwards, R.L., 1995a, Paleoclimate implications of mass spectrometric dating of a British flowstone: Geology, v. 23, p. 309–312.

Baker, A., Smart, P.L., Barnes, W.L., Edwards, R.L., and Farrant, A., 1995b, The Hekla 3 volcanic eruption recorded in a Scottish speleothem?: The Holocene, v. 5, p. 336–342.

Baker, A., Smart, P.L., and Edwards, R.L., 1996, Mass spectrometric dating of flowstones from Stump Cross Caverns and Lancaster Hole, Yorkshire: Palaeoclimate implications: Journal of Quaternary Sciences, v. 11, p. 107–114.

Baker, A., Genty, D., Dreybrodt, W., Barnes, W.L., Mockler, N.J., and Grapes, J., 1998, Testing theoretically predicted stalagmite growth rates with Recent annually laminated samples: Implications for past stalagmite deposition: Geochimica et Cosmochimica Acta, v. 62, p. 393–404.

Banner, J.L., Wasserburg, G.J., Chen, J.H., and Humphrey, J.D., 1991, Uranium-series evidence on diagenesis and hydrology in Pleistocene carbonates of Barbados, West Indies: Earth and Planetary Science Letters, v. 107, p. 129–137.

Banner, J.L., Musgrove, M., Asmeron, Y., Edwards, R.L., and Hoff, J.A., 1996, High-resolution temporal record of Holocene ground-water chemistry: Tracing links between climate and hydrology: Geology, v. 24, p. 1049–1053.

Bar-Matthews, M., Ayalon, A., and Kaufman, A., 1997,

Late Quaternary climate in the eastern Mediterranean region—Inferences from the stable isotope systematics of speleothems of the Soreq cave (Israel): Quaternary Research, v. 47, p. 155–168.

Bar-Matthews, M., Ayalon, A., Kaufman, A., and Wasserburg, G.J., 1999, The eastern Mediterranean paleoclimate as a reflection of regional events: Soreq Cave, Israel: Earth and Planetary Science Letters, v. 166, p. 85–95.

Bard, E., Hamelin, B., Fairbanks, R.G., and Zindler, A., 1990, Calibration of the ^{14}C time-scale over the last 30,000 years using mass spectrometric U-Th ages from Barbados corals: Nature, v. 31, p. 405–409.

Benson, L., and Thompson, R.S., 1987, The physical record of lakes in the Great Basin, *in* Ruddiman, W.F., and Wright, H.E., Jr., eds., North America and adjacent oceans during the last deglaciation: Boulder, Colorado, Geological Society of America, Geology of North America, v. K-3, p. 241–260.

Benson, L.V., Currey, D.R., Dorn, R.I., Lajoie, K.R., Oviatt, C.G., Robinson, S.W., Smith, G.I., and Stine, S., 1990, Chronology of expansion and contraction of four Great Basin lake systems during the past 35,000 years: Palaeogeography, Palaeoclimatology, Palaeoecology, v. 78, p. 241–286.

Berger, A., and Loutre, M.F., 1991, Insolation values for the last 10 million years: Quaternary Science Reviews, v. 10, p. 297–317.

Blum, M.D., Toomey, R.S., III, and Valastro, S., Jr., 1994, Fluvial response to late Quaternary climatic and environmental change, Edwards Plateau, Texas: Palaeogeography, Palaeoclimatology, Palaeoecology, v. 108, p. 1–21.

Broccoli, A.J., 2000, Tropical cooling at the Last Glacial Maximum: An atmosphere-mixed layer ocean model simulation: Journal of Climate, v. 13, p. 951–976.

Broecker, W.S., 1963, A preliminary evaluation of uranium series inequilibrium as a tool for absolute age measurements on marine carbonates: Journal of Geophysical Research, v. 68, p. 2817–2834.

Broecker, W.S., and Peng, T.-H., 1983, Tracers in the sea: Palisades, New York, Lamont-Doherty Geological Observatory, Columbia University, 690 p.

Brook, G.A., Burney, D.A., and Cowart, J.B., 1990, Desert paleoenvironmental data from cave speleothems with examples from the Chihuahuan, Somali-Chalbi, and Kalahari deserts: Palaeogeography, Palaeoclimatology, Palaeoecology, v. 76, p. 311–329.

Bryant, V.M., Jr., and Holloway, R.G., 1985, A late-Quaternary paleoenvironmental record of Texas: An overview of the pollen evidence, *in* Bryant, V.M., Jr., and Holloway, R.G., eds., Pollen record of late Quaternary North American sediments: Calgary, Canada, American Association of Stratigraphic Palynologists, p. 39–70.

Buhmann, D., and Dreybrodt, W., 1985a, The kinetics of calcite dissolution and precipitation in geologically relevant situations of karst areas, 1. Open system: Chemical Geology, v. 48, p. 189–211.

Buhmann, D., and Dreybrodt, W., 1985b, The kinetics of calcite dissolution and precipitation in geologically relevant situations of karst areas, 2. Closed system: Chemical Geology, v. 53, p. 109–124.

Burchett, C.R., Rettman, P.L., and Boning, C.W., 1986, The Edwards aquifer—Extremely productive, but . . . A sole-source water supply for San Antonio and surrounding counties in south-central Texas: San Antonio, Texas, U.S. Geological Survey and Edwards Underground Water District, 38 p.

Carter, W.T., 1931, The soils of Texas: College Station, Texas, Texas Agricultural Experiment Station Bulletin 431, 192 p.

Chen, J.H., Edwards, R.L., and Wasserburg, G.J., 1986, ^{238}U, ^{234}U and ^{232}Th in seawater: Earth and Planetary Science Letters, v. 80, p. 241–251.

Chen, J.H., Curran, H.A., White, B., and Wasserburg, G.J., 1991, Precise chronology of the last interglacial period ^{234}U-^{230}Th data from fossil coral reefs in the Bahamas: Geological Society of America Bulletin, v. 103, p. 82–97.

Cheng, H., Edwards, R.L., Murrell, M.T., and Benjamin, T.M., 1998, Uranium-thorium-protactinium dating systematics: Geochimica et Cosmochimica Acta, v. 62, p. 3437–3452.

Cheng, H., Edwards, R.L., Hoff, J., Gallup, C.D., Richards, D.A., and Asmeron, Y., 2000, The half-lives of uranium-234 and thorium-230: Chemical Geology, v. 169, p. 17–33.

COHMAP Members, 1988, Climatic changes of the last 18,000 years: Observations and model simulations: Science, v. 241, p. 1043–1052.

Dorale, J.A., Gonzalez, L.A., Reagan, M.K., Pickett, D.A., Murrell, M.T., and Baker, R.G., 1992, A high-resolution record of Holocene climate change in speleothem calcite from Cold Water Cave, northeast Iowa: Science, v. 258, p. 1626–1630.

Dorale, J.A., Edwards, R.L., Ito, E., and González, L.A., 1998, Climate and vegetation history of the mid-continent from 75 to 25 ka: A speleothem record from Crevice Cave, Missouri, USA: Science, v. 282, p. 1871–1874.

Dreybrodt, W., 1980, Deposition of calcite from thin films of natural calcareous solutions and the growth of speleothems: Chemical Geology, v. 29, p. 89–105.

Edwards, R.L., Chen, J.H., and Wasserburg, G.J., 1987, ^{238}U–^{234}U–^{230}Th–^{232}Th systematics and the precise measurement of time over the past 500,000 years: Earth and Planetary Science Letters, v. 81, p. 175–192.

Edwards, R.L., Beck, J.W., Burr, G.S., Donahue, D.J., Chappell, J.M.A., Bloom, A.L., Druffel, E.R.M., and Taylor, F.W., 1993, A large drop in atmospheric $^{14}C/^{12}C$ and reduced melting in the Younger Dryas, documented with ^{230}Th ages of corals: Science, v. 260, p. 962–968.

Edwards, R.L., Cheng, H., Murrell, M.T., and Goldstein, S.J., 1997, Protactinium-231 dating of carbonates by thermal ionization mass spectrometry: Implications for Quaternary climate change: Science, v. 276, p. 782–786.

Elliott, W.R., and Veni, G., eds., 1994, The caves and karst of Texas—1994 NSS Convention guidebook: Huntsville, Alabama, National Speleological Society, 342 p.

Eubanks, J.K., Cowart, J.B., Brook, G.A., Ellwood, B.B., 1985, Evidence for an increase in precipitation in S.E. New Mexico during cooler Quaternary climates: Chronology of a Carlsbad Cavern speleothem: Geological Society of America Abstracts with Program, v. 17, p. 576.

Frisia, S., Borsato, A., Fairchild, I.J., and McDermott, F., 2000, Calcite fabrics, growth mechanisms, and environments of formation in speleothems from the Italian Alps and southwestern Ireland: Journal of Sedimentary Research, v. 70, p. 1183–1196.

Gallup, C.D., Edwards, R.L., and Johnson, R.G., 1994, The timing of high sea levels over the past 200,000 years: Science, v. 263, p. 796–800.

Gascoyne, M., 1992, Palaeoclimate determination from cave calcite deposits: Quaternary Science Reviews, v. 11, p. 609–632.

Gascoyne, M., Schwarcz, H.P., and Ford, D.C., 1983, Uranium series ages of speleothems from north West England: Correlation with Quaternary climate: Philosophical Transactions of the Royal Society of London, ser. B, v. 301, p. 143–164.

Genty, D., and Quinif, Y., 1996, Annually laminated sequences in the internal structure of some Belgian stalagmites—Importance for paleoclimatology: Journal of Sedimentary Research, v. 66, p. 275–288.

Godfrey, C.L., McKee, G.S., and Oakes, H., 1973, General soil map of Texas: Texas Agricultural Experimental Station, Texas A&M University, in cooperation with the Soil Conservation Service, U.S. Department of Agriculture, scale 1:500 000, 2 sheets.

Goldstein, S.J., Murrell, M.T., Janecky, D.R., Delaney, J.R., and Clague, D.A., 1991, Geochronology and petrogenesis of MORB from the Juan de Fuca and Gorda ridges by ^{238}U–^{230}Th disequilibrium: Earth and Planetary Science Letters, v. 107, p. 25–41.

Gordon, D., Smart, P.L., Ford, D.C., Andrews, J.N., Atkinson, T.C., Rowe, P.J., and Christopher, N.S.J., 1989, Dating of late Pleistocene interglacials and interstadial periods in the United Kingdom from speleothem growth frequency: Quaternary Research, v. 31, p. 14–26.

Griffiths, J.F., and Strauss, R.F., 1985, The variety of Texas weather: Weatherwise, v. 38, p. 137–141.

Hennig, G.J., Grün, R., and Brunnacker, K., 1983, Speleothems, travertines, and paleoclimates: Quaternary Research, v. 20, p. 1–29.

Hill, C., and Forti, P., 1997, Cave minerals of the world (second edition): Huntsville, Alabama, National Speleological Society, 463 p.

Holland, H.D., Kirsipu, T.W., Huebner, J.S., and Oxburgh, U.M., 1964, On some aspects of the chemical evolution of cave waters: Journal of Geology, v. 72, p. 36–67.

Humphrey, J.D., and Ferring, C.R., 1994, Stable isotopic evidence for latest Pleistocene and Holocene climatic change in north-central Texas: Quaternary Research, v. 41, p. 200–213.

Imbrie, J., Hays, J.D., Martinson, D.G., McIntyre, A., Mix, A.C., Morley, J.J., Pisias, N.G., Prell, W.L., and Shackleton, N.J., 1984, The orbital theory of Pleistocene climate: Support from a revised chronology of the marine $\delta^{18}O$ record, *in* Berger, A., Imbrie, J., Hayes, J., Kukla, G., and Saltzman, B., eds., Milankovitch and climate: Dordrecht, Holland, D. Reidel Publishing Company, p. 269–305.

Ivanovich, M., and Harmon, R.S., eds., 1992, Uranium-series disequilibrium: Applications to earth, marine, and environmental sciences (second edition): Oxford, U.K., Oxford University Press, 910 p.

Jaffey, A.H., Flynn, K.F., Glendenin, L.E., Bentley, W.C., and Essling, A.M., 1971, Precision measurement of half-lives and specific activities of ^{235}U and ^{238}U: Physical Review C, v. 4, p. 1889–1906.

Jouzel, J., Barkov, N.I., Barnola, J.M., Bender, M., Cahppellaz, J., Genthon, C., Kotlyakov, V.M., Lipenkov, V., Lorius, C., Petit, J.R., Raynaud, D., Raisbeck, G., Ritz, C., Sowers, T., Stievenard, M., Yiou, F., and Yiou, P., 1993, Extending the Vostok ice-core record of palaeoclimate to the penultimate glacial period: Nature, v. 364, p. 407–412.

Kier, R.S., Garner, L.E., and Brown, L.F., Jr., 1977, Land resources of Texas: Austin, University of Texas Bureau of Economic Geology Land Resources Laboratory Series 2, 42 p.

Ku, T.-L., 1968, Protactinium-231 method of dating coral from Barbados Island: Journal of Geophysical Research, v. 73, p. 2271–2276.

Kutzbach, J.E., and Guetter, P.J., 1986, The influence of changing orbital parameters and surface boundary conditions on climate simulations for the past 18,000 years: Journal of the Atmospheric Sciences, v. 43, p. 1726–1759.

Kutzbach, J.E., and Wright, H.E., Jr., 1985, Simulation of the climate of 18,000 years BP: Results for the North American/North Atlantic/European sector and comparison with the geologic record of North America: Quaternary Science Reviews, v. 4, p. 147–187.

Lamothe, M., Parent, M., and Shilts, W.W., 1992, Sangamonian and early Wisconsinan events in the St. Lawrence Lowland and Appalachians of southern Quebec, Canada., *in* Clark, P.U., and Lea, P.D., eds., The last interglacial-glacial transition in North America: Geological Society of America Special Paper 270, p. 171–184.

Larkin, T.J., and Bomar, G.W., 1983, Climatic atlas of Texas: Austin, Texas Department of Water Resources, 151 p.

Li, W.-X., Lundberg, J., Dickin, A.P., Ford, D.C., Schwarcz, H.P., McNutt, R., and Williams, D., 1989, High-precision mass-spectrometric uranium-series dating of cave deposits and implications for palaeoclimate studies: Nature, v. 339, p. 524–536.

Manabe, S., and Broccoli, A.J., 1985, The influence of continental ice sheets on the climate of an ice age: Journal of Geophysical Research, v. 90D, p. 2167–2190.

McMahan, C.A., Frye, R.G., and Brown, K.L., 1984, The vegetation types of Texas including cropland: Austin, Texas Parks and Wildlife Department, Wildlife Division, 40 p.

Musgrove, M., 2000, Temporal links between climate and hydrology: Insights from central Texas cave deposits and groundwater [Ph.D. thesis]: Austin, University of Texas, 432 p.

Nordt, L.C., Boutton, T.W., Hallmark, C.T., and Waters,

M.R., 1994, Late Quaternary vegetation and climatic changes in central Texas based on the isotopic composition of organic carbon: Quaternary Research, v. 41, p. 109–120.

Oviatt, C.G., and McCoy, W.D., 1992, Early Wisconsin lakes and glaciers in the Great Basin, U.S.A., *in* Clark, P.U., and Lea, P.D., eds., The last interglacial-glacial transition in North America: Geological Society of America Special Paper 270, p. 279–287.

Pearson, F.J., Jr., Rettman, P.L., and Wyerman, T.A., 1975, Environmental tritium in the Edwards aquifer, central Texas, 1963–1971: U.S. Geological Survey Open-File Report 74–362, 32 p.

Petit, J.R., Mounier, L., Jouzel, J., Korotkevich, Y.S., Kotlyakov, V.I., and Lorius, C., 1990, Palaeoclimatological and chronological implications of the Vostok core dust record: Nature, v. 343, p. 56–58.

Phillips, F.M., Zreda, M.G., Smith, S.S., Elmore, D., Kubik, P.W., and Sharma, P., 1990, Cosmogenic chlorine-36 chronology for glacial deposits at Bloody Canyon, eastern Sierra Nevada: Science, v. 248, p. 1529–1532.

Phillips, F.M., Campbell, A.R., Kruger, C., Johnson, P., Roberts, R., and Keyes, E., 1992, A reconstruction of the response of the water balance in western United States lake basins to climatic change, Volume 1: Las Cruces, New Mexico Water Resources Research Institute Report 269, 167 p.

Phillips, F.M., Campbell, A.R., Smith, G.I., and Bischoff, J.L., 1994, Interstadial climatic cycles: A link between western North America and Greenland?: Geology, v. 22, p. 1115–1118.

Pickett, D.A., Murrell, M.T., and Williams, R.W., 1994, Determination of femtogram quantities of protactinium in geologic samples by thermal ionization mass spectrometry: Analytical Chemistry, v. 66, p. 1044–1049.

Puente, C., 1975, Relation of precipitation to annual ground-water recharge in the Edwards aquifer, San Antonio area, Texas: U.S. Geological Survey Open-File Report 75–298, 31 p.

Raich, J.W., and Potter, C.S., 1995, Global patterns of carbon dioxide emissions from soils: Global Biogeochemical Cycles, v. 9, p. 23–36.

Raich, J.W., and Schlesinger, W.H., 1992, The global carbon dioxide flux in soil respiration and relationship to vegetation and climate: Tellus, v. 44B, p. 81–89.

Railsback, L.B., Brook, G.A., Chen, J., Kalin, R., and Fleisher, C.J., 1994, Environmental controls on the petrology of a late Holocene speleothem from Botswana with annual layers of aragonite and calcite: Journal of Sedimentary Research, v. A64, p. 147–155.

Reeves, C.C., Jr., 1973, The full glacial climate of the southern High Plains, west Texas: Journal of Geology, v. 81, p. 693–704.

Rind, D., 1987, Components of the ice age circulation: Journal of Geophysical Research, v. 90D, p. 4241–4281.

Robert, J., Miranda, C.F., and Muxart, R., 1969, Mesure de la période du protactinium 231 par microcalorimétrie: Radiochimica Acta, v. 11, p. 104–108.

Schwarcz, H.P., and Latham, A.G., 1989, Dirty calcites, 1. Uranium-series dating of contaminated calcite using leachates alone: Chemical Geology, Isotope Geoscience Section, v. 80, p. 35–43.

Shopov, Y.Y., Ford, D.C., Schwarcz, H.P., 1994, Luminescent microbanding in speleothems: High-resolution chronology and paleoclimate: Geology, v. 22, p. 407–410.

Smart, P.L., and Friederich, H., 1986, Water movement and storage in the unsaturated zone of a maturely karstified aquifer, Mendip Hills, England, *in* Proceedings of the Environmental Problems in Karst Terrains and their Solutions Conference, Bowling Green, KY: Dublin, Ohio, National Water Well Association, p. 59–87.

Smith, G.I., and Street-Perrott, F.A., 1983, Pluvial lakes of the western United States, *in* Porter, S.C., ed., Late-Quaternary environments of the United States, Volume 1, The late Pleistocene: Minneapolis, University of Minnesota Press, p. 190–214.

Stirling, C.H., Esat, T.M., McCulloch, M.T., and Lambeck, K., 1995, High-precision U-series dating of corals from Western Australia and implications for the timing and duration of the last interglacial: Earth and Planetary Science Letters, v. 135, p. 115–130.

Stute, M., Schlosser, P., Clark, J.F., and Broecker, W.S., 1992, Paleotemperatures in the southwestern United States derived from noble gases in groundwater: Science, v. 256, p. 1000–1003.

Szabo, B.J., 1990, Ages of travertine deposits in eastern Grand Canyon National Park, Arizona: Quaternary Research, v. 34, p. 24–32.

Szabo, B.J., Kolesar, P.T., Riggs, A.C., Winograd, I.J., and Ludwig, K.R., 1994, Paleoclimatic inferences from a 120,000-yr calcite record of water-table fluctuation in Browns Room of Devils Hole, Nevada: Quaternary Research, v. 41, p. 59–69.

Thompson, R.S., Whitlock, C., Bartlein, P.J., Harrison, S.P., and Spaulding, W.G., 1993, Climatic changes in the western United States since 18,000 yr B.P., *in* Wright, H.E., Jr., Kutzbach, J.E., Webb, T., III, Ruddiman, W.F., Street-Perrott, F.A., and Bartlein, P.J., eds., Global climates since the Last Glacial Maximum: Minneapolis, University of Minnesota Press, p. 468–513.

Toomey, R.S., III, Blum, M.D., and Valastro, S., Jr., 1993, Late Quaternary climates and environments of the Edwards Plateau, Texas: Global and Planetary Change, v. 7, p. 299–320.

Waters, M.R., and Nordt, L.C., 1995, Late Quaternary floodplain history of the Brazos River in east-central Texas: Quaternary Research, v. 43, p. 311–319.

Whitehead, N.E., Ditchburn, R.G., Williams, P.W., McCabe, W.J., 1999, ^{231}Pa and ^{230}Th contamination at zero age; a possible limitation on U/Th series dating of speleothem material: Chemical Geology, v. 156, p. 359–366.

Wilkens, D.E., and Currey, D.R., 1997, Timing and extent of late Quaternary paleolakes in the Trans-Pecos closed basin, west Texas and south-central New Mexico: Quaternary Research, v. 47, p. 306–315.

Winograd, I.J., Szabo, B.J., Coplen, T.B., and Riggs, A.C., 1988, A 250,000-year climatic record from Great Basin vein calcite: Implications for Milankovitch theory: Science, v. 242, p. 1275–1280.

Winograd, I.J., Coplen, T.B., Landwehr, J.M., Riggs, A.R., Ludwig, K.R., Szabo, B.J., Kolesar, P.T., and Revesz, K.M., 1992, Continuous 500,000-year climate record from vein calcite in Devils Hole, Nevada: Science, v. 258, p. 255–260.

MANUSCRIPT RECEIVED BY THE SOCIETY JUNE 26, 2000
REVISED MANUSCRIPT RECEIVED APRIL 23, 2001
MANUSCRIPT ACCEPTED MAY 9, 2001

Printed in the USA